Journal of Computational and Applied Mathematics 235 (2011) 2234–2241

Contents lists available at ScienceDirect

Journal of Computational and Applied Mathematics

journal homepage: www.elsevier.com/locate/cam

A novel variational model for image segmentation☆

Yanli Zhai, Dazhi Zhang*, Jiebao Sun, Boying Wu

Department of Mathematics, Harbin Institute of Technology, Harbin 150001, PR China

ARTICLE INFO

Article history:
Received 20 July 2009
Received in revised form 12 June 2010

Keywords:
Image segmentation
Ginzburg–Landau model
Semi-norm

ABSTRACT

In this paper, we propose a new variational model for image segmentation. Our model is inspired by the complex Ginzburg–Landau model and the semi-norm defined by us. This new model can detect both the convex and concave parts of images. Moreover, it can also detect non-closed edges as well as quadruple junctions. Compared with other methods, the initialization is completely automatic and the segmented images obtained by using our new model could keep fine structures and edges of the original images very effectively. Finally, numerical results show the effectiveness of our model.

1. Introduction

Variational methods have been extensively studied in image segmentation and denoising because of their flexibility in modeling and various advantages in the numerical implementation. The basic idea of variational methods is to minimize an energy functional. This functional generally depends on the features of images. The classical way to solve the minimization problem is to solve the corresponding Euler–Lagrange equation or its associated flow.

There are many variational models for image segmentation which can be categorized into two classes: edge-based models [1–4] and region-based models [5–7]. Edge-based models utilize the image gradient to stop evolving contours on object boundaries such as the geodesic active contour (GAC) model [2]. But there may be some disadvantages, for instance, the energy may evolve to its bad local minimum for a given initial curve. Region-based models have some advantages over edge-based models: Firstly, region-based models do not utilize the image gradient, so they have better performance for images with weak boundaries; Secondly, these models are significantly less sensitive to the location of initial contours. One can take the Chan–Vese (CV) model [8] or the region-scalable fitting model [9] as an example. The CV model is successful for an image with two regions, each of which has a distinct mean of pixel intensities. But the CV model is not applicable to images with intensity inhomogeneity. To deal with a more general situation, Chunming Li proposed the region-scalable fitting model to handle images with intensity inhomogeneity in [9]. In numerical experiments of the edge-based and region-based models, the level set method is usually used, but this method is computationally expensive since it works in a higher dimension space than the image space itself.

In this paper, we propose a new variational model for image segmentation. This new model is inspired by the complex Ginzburg–Landau (GL) model [10,11] which can be used to model many phenomena in physics, especially in the theory of superconductors. This GL model has an important property that it is able to distinguish the normal phases and superconducting phases of materials. While we use it for image segmentation, almost all of the obvious edges could be detected because the edges correspond to normal phases and other regions correspond to superconducting phases. However, owing to the existence of a Sobolev semi-norm, segmented images may lose some weak edges and important details.

☆ This work is supported by "the Fundamental Research Funds for the Central Universities" (Grant No. HIT. NSRIF. 2009049), and also supported by Natural Sciences Foundation of Heilongjiang Province (A200909).

* Corresponding author.
E-mail address: zhang-d-z@163.com (D. Zhang).

0377-0427/$ – see front matter © 2010 Elsevier B.V. All rights reserved.
doi:10.1016/j.cam.2010.10.020

In order to overcome this shortcoming, we replace this Sobolev semi-norm with a new semi-norm defined by us which is a variant of the non-local bounded variation regularization [12–17]. This new semi-norm has many important properties that enable fine structures and edges to be detected very well when it is used in image segmentation. Moreover, a fidelity term is also added to our new model since it is very useful for preserving the significant information of original images. Therefore, our model can detect both the convex and concave parts of images. Furthermore, it can detect non-closed edges as well as quadruple junctions too. Compared with other active contours methods, the initialization is completely automatic and the segmented images obtained by using our new model can perform better.

The remainder of the paper is organized as follows: in Section 2, we give the definition and some properties of the new semi-norm. In Section 3, our new model is proposed. In Section 4, the corresponding Euler–Lagrange equation or its associated flow is obtained. And the iterating schemes are also given in this section. In Section 5, we give some experimental results. Finally, we conclude our paper in Section 6.

2. Definitions and notations

In this paper, we extend the NLBV_τ norm [13] to a new norm firstly. In the following, let Ω be a bounded open subset of $\mathbb{R}^2$ and $u : \Omega \mapsto \mathbb{R}$ be a function.

Definition 2.1. Assume $u \in L^1(\Omega)$ and g is a nonnegative function. We define $u \in g - \mathrm{NLBV}_\tau(\Omega)$, if u satisfies

$$\begin{aligned} |u|_{g-\mathrm{NLBV}_\tau(\Omega)} &= \sup_{\phi}\left\{\int_X u(x)\big(\mathrm{div}_x\phi(x,y) - \mathrm{div}_x\phi(y,x)\big)\mathrm{d}x\mathrm{d}y : \phi \in V\right\} \\ &< \infty, \end{aligned} \tag{2.1}$$

where $X = \{(x,y) \in \Omega \times \Omega, |x-y| < \tau\}$, $V = \{\phi \in C_0^1(X), |\phi(x,y)| \le g(x)g(y)\}$. The norm of this space can be defined as follows

$$\|u\|_{g-\mathrm{NLBV}_\tau(\Omega)} = |u|_{g-\mathrm{NLBV}_\tau(\Omega)} + \|u\|_{L^1(\Omega)}.$$

The space of all functions $u \in g - \mathrm{NLBV}_\tau(\Omega)$ is a Banach space. $|u|_{g-\mathrm{NLBV}_\tau(\Omega)}$ is called the $g - \mathrm{NLBV}_\tau$ semi-norm of u.

If $u \in W^{1,1}(\Omega)$, we know

$$\begin{aligned} |u|_{g-\mathrm{NLBV}_\tau(\Omega)} &= \sup_{\phi}\left\{\int_X u(x)\big(\mathrm{div}_x\phi(x,y) - \mathrm{div}_x\phi(y,x)\big)\mathrm{d}x\mathrm{d}y : \phi \in V\right\} \\ &= \sup_{\phi}\left\{\int_X (\nabla u(x) - \nabla u(y))\cdot\phi(x,y)\mathrm{d}x\mathrm{d}y : \phi \in V\right\} \\ &= \int_X g(x)g(y)|\bigtriangledown u(x) - \bigtriangledown u(y)|\mathrm{d}x\mathrm{d}y, \end{aligned}$$

where $X = \{(x,y) \in \Omega \times \Omega, |x-y| < \tau\}$ is a bounded open set and $g(x)g(y)$ is the weighted function defined on the domain X in essence.

Proposition 2.1 (*The Lower Semi-continuity*). *Let $\{u_n\}$ be a sequence in the space $g - \mathrm{NLBV}_\tau(\Omega)$, if $u_n \to u$ strongly in $L^1(\Omega)$ and $u \in g - \mathrm{NLBV}_\tau(\Omega)$, then*

$$|u|_{g-\mathrm{NLBV}_\tau(\Omega)} \le \lim_{n\to\infty}\inf |u_n|_{g-\mathrm{NLBV}_\tau(\Omega)}.$$

Proof. For $\forall\phi \in C_0^1(X)$, $|\phi(x,y)| \le g(x)g(y)$, we have

$$\begin{aligned} \int_X u(x)\big(\mathrm{div}_x\phi(x,y) - \mathrm{div}_x\phi(y,x)\big)\mathrm{d}x\mathrm{d}y &= \lim_{n\to\infty}\int_X u_n(x)\big(\mathrm{div}_x\phi(x,y) - \mathrm{div}_x\phi(y,x)\big)\mathrm{d}x\mathrm{d}y \\ &\le \lim_{n\to\infty}\inf\sup_{\phi}\left\{\int_X u_n(x)\big(\mathrm{div}_x\phi(x,y) - \mathrm{div}_x\phi(y,x)\big)\mathrm{d}x\mathrm{d}y\right\} \\ &\le \lim_{n\to\infty}\inf |u_n|_{g-\mathrm{NLBV}_\tau(\Omega)}. \end{aligned}$$

Taking the supremum over $V = \{\phi \in C_0^1(X), |\phi(x,y)| \le g(x)g(y)\}$, we conclude that

$$|u|_{g-\mathrm{NLBV}_\tau(\Omega)} \le \lim_{n\to\infty}\inf |u_n|_{g-\mathrm{NLBV}_\tau(\Omega)}. \quad \square$$

In the following, we discuss the relationship between the $g - \mathrm{NLBV}_\tau$ semi-norm and the BV semi-norm.

Proposition 2.2. *If $u \in g - \mathrm{NLBV}_\tau(\Omega)$ and $0 < \beta^2 \le g(x)g(y) \le 1$, then we can obtain*

$$\beta^2|u|_{\mathrm{NLBV}_\tau(\Omega)} \le |u|_{g-\mathrm{NLBV}_\tau(\Omega)} \le |u|_{\mathrm{NLBV}_\tau(\Omega)},\ |u|_{g-\mathrm{NLBV}_\tau(\Omega)} \le c(\Omega)|u|_{\mathrm{BV}(\Omega)},$$

where $c(\Omega)$ is a constant that only depends on the domain Ω.

Proof. It is known to all that

$$V_\beta \subset V \subset V_1,$$

where $V_\beta = \{\phi \in C_0^1(X), |\phi(x,y)| \le \beta^2\}$, $V = \{\phi \in C_0^1(X), |\phi(x,y)| \le g(x)g(y)\}$, $V_1 = \{\phi \in C_0^1(X), |\phi(x,y)| \le 1\}$.

From the definition of NLBV_τ semi-norm [13], we easily obtain the following results

$$\begin{aligned}\beta^2|u|_{\mathrm{NLBV}_\tau(\Omega)} &= \beta^2 \sup_\phi \left\{\int_X u(x)\big(\mathrm{div}_x\phi(x,y) - \mathrm{div}_x\phi(y,x)\big)\mathrm{d}x\mathrm{d}y : \phi \in V_1\right\}\\ &= \sup_\phi \left\{\int_X u(x)\big(\mathrm{div}_x(\beta^2\phi(x,y)) - \mathrm{div}_x(\beta^2\phi(y,x))\big)\mathrm{d}x\mathrm{d}y : \phi \in V_1\right\}.\end{aligned}$$

Let $\beta^2\phi(x,y) = \psi(x,y)$, then $\beta^2\phi(y,x) = \psi(y,x)$.

Since $\forall\phi \in V_1$, we can get $\psi \in V_\beta$. Besides, for any $\psi \in V_\beta$, we can choose a $\phi \in V_1$ s.t. $\psi = \beta^2\phi$. Then

$$\begin{aligned}\beta^2|u|_{\mathrm{NLBV}_\tau(\Omega)} &= \sup_\phi \left\{\int_X u(x)\big(\mathrm{div}_x\psi(x,y) - \mathrm{div}_x\psi(y,x)\big)\mathrm{d}x\mathrm{d}y : \psi = \beta^2\phi, \phi \in V_1\right\}\\ &= \sup_\psi \left\{\int_X u(x)\big(\mathrm{div}_x\psi(x,y) - \mathrm{div}_x\psi(y,x)\big)\mathrm{d}x\mathrm{d}y : \psi \in V_\beta\right\}\\ &\le \sup_\psi \left\{\int_X u(x)\big(\mathrm{div}_x\psi(x,y) - \mathrm{div}_x\psi(y,x)\big)\mathrm{d}x\mathrm{d}y : \psi \in V\right\}\\ &= |u|_{g-\mathrm{NLBV}_\tau(\Omega)}.\end{aligned}$$

And by the formula $V \subset V_1$ and the definitions of (2.1) and NLBV_τ semi-norm, we can also get

$$|u|_{g-\mathrm{NLBV}_\tau(\Omega)} \le |u|_{\mathrm{NLBV}_\tau(\Omega)}.$$

Moreover, we know

$$\begin{aligned}|u|_{\mathrm{NLBV}_\tau(\Omega)} &= \sup_\phi \left\{\int_X u(x)\big(\mathrm{div}_x\phi(x,y) - \mathrm{div}_x\phi(y,x)\big)\mathrm{d}x\mathrm{d}y : \phi \in V_1\right\}\\ &\le 2\sup_\phi \left\{\int_X u(x)\mathrm{div}_x\phi(x,y)\mathrm{d}x\mathrm{d}y : \phi \in V_1\right\}\\ &\le 2\sup_\phi \left\{\int_\Omega u(x)\int_{\Omega_x}\mathrm{div}_x\big(\phi(x,y)\big)\mathrm{d}y\mathrm{d}x : \phi \in V_1\right\},\end{aligned}$$

where $V_1 = \{\phi \in C_0^1(X) : |\phi(x,y)| \le 1\}$, $\Omega_x = \{y \in \Omega : |x-y| < \tau\}$.

Since $\phi \in C_0^1(X)$, we can obtain

$$|u|_{\mathrm{NLBV}_\tau(\Omega)} \le 2\sup_\phi \left\{\int_\Omega u(x)\mathrm{div}_x\left(\int_{\Omega_x}\phi(x,y)\mathrm{d}y\right)\mathrm{d}x : \phi \in V_1\right\}.$$

Let

$$\theta(x) = \frac{\int_{\Omega_x}\phi(x,y)\mathrm{d}y}{\sqrt{2}|\Omega|}$$

we know $|\theta(x)| \le 1$.

Since $\phi \in C_0^1(X)$, we can obtain that $\theta \in C_0^1(\Omega)$. Thus,

$$|u|_{\mathrm{NLBV}_\tau(\Omega)} \le 2\sqrt{2}|\Omega|\sup_\theta \left\{\int_\Omega u(x)\mathrm{div}\,\theta(x)\mathrm{d}x : \theta(x) \in \bar{V}\right\},$$

where $\bar{V} = \{\theta \in C_0^1(\Omega) : |\theta(x)| \le 1\}$.

Therefore,

$$|u|_{\mathrm{NLBV}_\tau(\Omega)} \le c(\Omega)|u|_{\mathrm{BV}(\Omega)}.$$

That is,

$$|u|_{g-\mathrm{NLBV}_\tau(\Omega)} \le c(\Omega)|u|_{\mathrm{BV}(\Omega)}$$

where $c(\Omega)$ is a constant that only depends on the domain Ω. □

From the above propositions, we know this new space shares many similar properties with the space of functions of bounded variation. Moreover, according to the observation, we find if $u \in W^{1,1}(\Omega)$, the gradient values of u in the τ neighbor domain of a point x are all considered in the new semi-norm defined by us. So when this new semi-norm is used in image segmentation, it is very useful for keeping fine structures and edges of images. In our paper, we use this semi-norm to construct a new model for image segmentation.

3. Our proposed model

The Ginzburg–Landau model has shown its efficiency for modeling many phenomena in physics, especially in the theory of superconductors [10,11]. The Ginzburg–Landau functional is defined as follows:

$$E_\varepsilon = \frac{1}{2}\int_\Omega \left(|\nabla u|^2 + \frac{1}{2\varepsilon^2}(1-|u|^2)^2\right)\mathrm{d}x,$$

where ε is a small constant, u is a complex-valued function indicating the local state of the material: if $|u| \approx 1$, the material is in a superconducting phase, while if $|u| \approx 0$, it is in its normal phase. Thus, the Ginzburg–Landau model is able to distinguish the normal and superconducting phases. In this paper, we let the edges correspond to the normal phases and other regions correspond to the superconducting phases. Hence, the edges could be detected.

Now, let $f : \Omega \subset \mathbb{R}^2 \to \mathbb{R}$ be the observed image. In order to apply the Ginzburg–Landau model, we should convert $f(x)$ into a complex-valued function u_0. To construct u_0, firstly we re-scale $f(x)$ to the interval $[-1, 1]$ by the formula $v_0 = \frac{2f(x)}{255} - 1$ and assume $w_0 = \sqrt{1-v_0^2}$. Then we define $\mathrm{Re}(u_0) = v_0$ and $\mathrm{Im}(u_0) = w_0$ so that $|u_0| = 1$. Compared with the construction of the initial level set function (where signed distance function is usually used) in the active contour methods, our initialization is easier and automatic.

Inspired by the complex Ginzburg–Landau model and the new semi-norm we define, we propose our new model by minimizing the following energy functional in $g - \mathrm{NLBV}_\tau(\Omega) \cap L^4(\Omega)$:

$$F(u) = \mu|u|_{g-\mathrm{NLBV}_\tau(\Omega)} + \frac{1}{4\varepsilon^2}\int_\Omega \left(1-|u|^2\right)^2\mathrm{d}x + \frac{\lambda}{2}\int_\Omega |u-u_0|^2\mathrm{d}x, \tag{3.1}$$

where the function $g(x)g(y)$ is defined as:

$$g(x)g(y) = \frac{1}{(1+\overline{\beta}|\nabla G_\sigma * f(x)|^2)} \cdot \frac{1}{(1+\overline{\beta}|\nabla G_\sigma * f(y)|^2)}, \tag{3.2}$$

where G_σ is the Gaussian function and $\overline{\beta}$ is a positive constant.

In the following, we should explain further why the proposed energy functional is defined as the formula (3.1):

(1) In the first term, the function $g(x)g(y)$ serves the purpose of selecting the locations of X to be smoothed. Obviously, if we choose $g(x)g(y)$ as the same as the formulas (3.2), edges could be kept very well.

(2) As analyzed in Section 2, when the $g - \mathrm{NLBV}_\tau$ semi-norm is used in image segmentation, it is very useful for keeping fine structures and edges of images. Therefore, our proposed model can perform very well.

(3) From the second term, it is derived that $|u| \approx 1$ almost everywhere after enough diffusion except for the points along the edges of objects, and $|u|$ is near zero along edges.

(4) The third term is a fidelity term which forces u to be a close approximation of the original function u_0.

4. Numerical implementation

Numerically, we use the following minimization problem instead of (3.1):

$$\min_{u\in W^{1,1}(\Omega)\cap L^4(\Omega)} \left\{F(u) = \mu\int_X g(x)g(y)\sqrt{|\nabla u(x)-\nabla u(y)|^2+\eta}\mathrm{d}x\mathrm{d}y + \frac{1}{4\varepsilon^2}\int_\Omega \left(1-|u|^2\right)^2\mathrm{d}x + \frac{\lambda}{2}\int_\Omega |u-u_0|^2\mathrm{d}x\right\}.$$

In the above formula, we use a small positive constant η to avoid the singulary. This process is the well-known ε-regularization. From the paper [18,13], it is known that Euler–Lagrange equations must be satisfied. Since this energy functional is uncommon, we must deduce the corresponding Euler–Lagrange equations firstly.

If $u(x)$ is a real function, Euler–Lagrange equations are:

$$\int_{\Omega_x} g(x)g(y)\frac{\nabla u(x)-\nabla u(y)}{\sqrt{|\nabla u(x)-\nabla u(y)|^2+\eta}}\mathrm{d}y \cdot n = 0, \quad x \in \partial\Omega, \tag{4.1}$$

where n is the outward unit normal to $\partial\Omega$.

$$-2\mu\mathrm{div}\left(\int_{\Omega_x} g(x)g(y)\frac{\nabla u(x)-\nabla u(y)}{\sqrt{|\nabla u(x)-\nabla u(y)|^2+\eta}}\mathrm{d}y\right)-\frac{1}{\epsilon^2}u(x)(1-|u(x)|^2)+\lambda(u-u_0)=0,\quad x\in\Omega, \tag{4.2}$$

where $\Omega_x=\{y\in\Omega:|x-y|<\tau\}$.

In this paper, u is a complex-valued function. We make $u=(v,w)$. According to the above analysis, we can get the similar Euler–Lagrange equations with the Eqs. (4.1)–(4.2).

In order to solve these equations, we use the steepest descent method. Therefore, we can get the following heat flows with respect to the real and imaginary part of the complex-valued function u:

(1) The heat flows with respect to v:

$$\frac{\partial v}{\partial t}=2\mu\mathrm{div}(r)+\frac{1}{\epsilon^2}v\big(1-(v^2+w^2)\big)-\lambda(v-v_0), \tag{4.3}$$

where $r(x)$ is defined as follows:

$$\int_{\Omega_x} g(x)g(y)\frac{\nabla v(x)-\nabla v(y)}{\sqrt{|\nabla v(x)-\nabla v(y)|^2+\eta+|\nabla w(x)-\nabla w(y)|^2}}\mathrm{d}y. \tag{4.4}$$

(2) The heat flows with respect to w:

$$\frac{\partial w}{\partial t}=2\mu\mathrm{div}(s)+\frac{1}{\epsilon^2}w\big(1-(v^2+w^2)\big)-\lambda(w-w_0), \tag{4.5}$$

where $s(x)$ is defined as follows:

$$\int_{\Omega_x} g(x)g(y)\frac{\nabla w(x)-\nabla w(y)}{\sqrt{|\nabla v(x)-\nabla v(y)|^2+\eta+|\nabla w(x)-\nabla w(y)|^2}}\mathrm{d}y. \tag{4.6}$$

The initial value u_0 of these equations is equal to (v_0, w_0) and the boundary condition is:

$$r(x)\cdot n=0,\quad x\in\partial\Omega, \tag{4.7}$$

and

$$s(x)\cdot n=0,\quad x\in\partial\Omega, \tag{4.8}$$

where the functions $r(x)$, $s(x)$ are defined as the same as the formulas (4.4), (4.6).

We use finite difference schemes to solve the Eqs. (4.3) and (4.5). Denote the space step by $h=1$ and the time step by t. Then we have

$$\begin{aligned}
&(D^+_{x_1}u)_{i,j}=u_{i+1,j}-u_{i,j},\qquad (D^-_{x_1}u)_{i,j}=u_{i,j}-u_{i-1,j},\\
&(D^+_{x_2}u)_{i,j}=u_{i,j+1}-u_{i,j},\qquad (D^-_{x_2}u)_{i,j}=u_{i,j}-u_{i,j-1},\\
&|(Du)_{i,j}-(Du)_{l,k}|=\sqrt{((D^+_{x_1}u)_{i,j}-(D^+_{x_1}u)_{l,k})^2+((D^+_{x_2}u)_{i,j}-(D^+_{x_2}u)_{l,k})^2}.
\end{aligned}$$

The iteration formulas are given by

$$\begin{aligned}
v^{n+1}_{i,j}&=v^n_{i,j}+t\Big(2\mu A^n_{i,j}+\frac{1}{\epsilon^2}v^n_{i,j}(1-(v^n_{i,j})^2-(w^n_{i,j})^2)-\lambda(v^n_{i,j}-v_0)\Big),\\
w^{n+1}_{i,j}&=w^n_{i,j}+t\Big(2\mu B^n_{i,j}+\frac{1}{\epsilon^2}w^n_{i,j}(1-(v^{n+1}_{i,j})^2-(w^n_{i,j})^2)-\lambda(w^n_{i,j}-w_0)\Big),
\end{aligned}$$

where

$$\begin{aligned}
A^n_{i,j}=&D^-_{x_1}\left(\sum_{l,k}g_{i,j}g_{l,k}\frac{(D^+_{x_1}v)^n_{i,j}-(D^+_{x_1}v)^n_{l,k}}{\sqrt{|(Dv)^n_{i,j}-(Dv)^n_{l,k}|^2+|(Dw)^n_{i,j}-(Dw)^n_{l,k}|^2+\eta}}\right)\\
&+D^-_{x_2}\left(\sum_{l,k}g_{i,j}g_{l,k}\frac{(D^+_{x_2}v)^n_{i,j}-(D^+_{x_2}v)^n_{l,k}}{\sqrt{|(Dv)^n_{i,j}-(Dv)^n_{l,k}|^2+|(Dw)^n_{i,j}-(Dw)^n_{l,k}|^2+\eta}}\right),
\end{aligned}$$

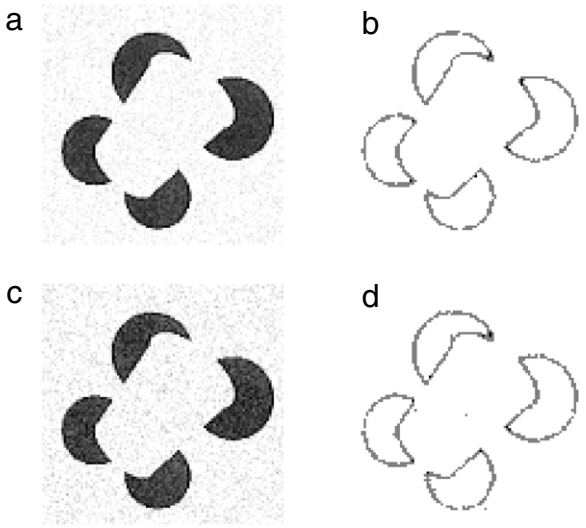

Fig. 1. An example of image segmentation: (a) The original noisy image with the Gaussian noise; (b) The segmented image obtained by using our new model (iteration $= 6$, $\gamma = 2$, $\tau = 13$); (c) The original noisy image with the Gaussian noise of a different variance; (d) The segmented image obtained by using our new model (iteration $= 6$, $\gamma = 2$, $\tau = 11$).

and

$$B^n_{i,j} = D^-_{x_1}\left(\sum_{l,k} g_{i,j}g_{l,k}\frac{(D^+_{x_1}w)^n_{i,j} - (D^+_{x_1}w)^n_{l,k}}{\sqrt{|(Dv)^n_{i,j} - (Dv)^n_{l,k}|^2 + |(Dw)^n_{i,j} - (Dw)^n_{l,k}|^2 + \eta}}\right) + D^-_{x_2}\left(\sum_{l,k} g_{i,j}g_{l,k}\frac{(D^+_{x_2}w)^n_{i,j} - (D^+_{x_2}w)^n_{l,k}}{\sqrt{|(Dv)^n_{i,j} - (Dv)^n_{l,k}|^2 + |(Dw)^n_{i,j} - (Dw)^n_{l,k}|^2 + \eta}}\right).$$

Moreover, we can also use finite difference schemes to solve the boundary conditions (4.7) and (4.8). According to the boundary conditions, we can get $D^+_{x_1}v^n(x)(or D^-_{x_1}v^n(x))$, $D^+_{x_1}w^n(x)$ (or $D^-_{x_1}w^n(x)$) when $x \in \partial\Omega$ and n is orthogonal to the x_2-axe. And we can also obtain $D^+_{x_2}v^n(x)$ (or $D^-_{x_2}v^n(x)$), $D^+_{x_2}w^n(x)$ (or $D^-_{x_2}v^n(x)$) when $x \in \partial\Omega$ and n is orthogonal to the x_1-axe.

5. Experimental results

The proposed variational method has been applied to a variety of synthetic and real gray images. We choose the parameters as $\varepsilon = 1$, $\lambda = 0.1$, $t = 0.1$.

In our experiments for gray images, we get v and w after evolution. The segmented image is displayed by $255(v^2+w^2)^\gamma$, where γ is chosen between 2 and 100 in this paper. The reason for using $255(v^2 + w^2)^\gamma$ is as follows: from the Section 3, we know u has the following property after enough diffusion: $|u| \approx 1$ in the smoothed regions and $|u|$ is near zero along edges. Thus,

$$255(v^2 + w^2)^\gamma \approx \begin{cases} 255, & \text{smoothed regions,} \\ 0, & \text{along edges.} \end{cases}$$

Therefore, as a result of segmentation, the edges are displayed in dark while the smoothed regions are in bright. Moreover, in our paper, τ is chosen to be not very large in order to compute our model efficiently. In general, if the background of an image is very simple, the value of τ can be chosen to be small. If the image is a noisy image, the value of τ can be chosen to be a bit larger. In our experiments, the maximal value of τ is 13 (e.g. in Fig. 1).

Firstly, we use our new model to deal with noisy images in Figs. 1 and 2. Figs. 1(a), (c) and 2(a) are the noisy images. The segmented images are shown in Figs. 1(b), (d) and 2(b). We find this model is able to detect both the convex and concave parts of noisy images very accurately. Then we use it to deal with images Figs. 3(a) and 4(a) that contain quadruple junctions. The experimental results show that our model can detect non-closed curves.

In Fig. 5(a), it is a synthetic image of a plane and the intensity of the background is heterogeneous. This situation is very common, but many methods may not perform very well. The model proposed by us could be used for the segmentation of this kind of image. The segmented image is shown in Fig. 5(b). We find our model can detect the edges and fine structures very well for this kind of image.

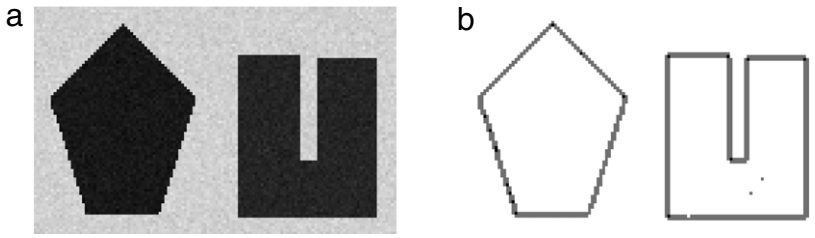

Fig. 2. An example of image segmentation: (a) The original noisy image with the Gaussian noise; (b) The segmented image obtained by using our new model (iteration $= 10$, $\gamma = 2$, $\tau = 7$).

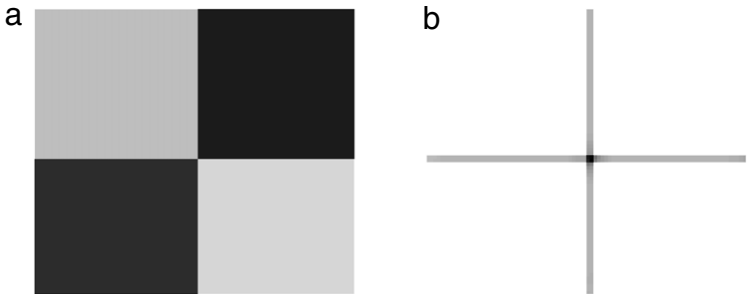

Fig. 3. An example of image segmentation: (a) The original image; (b) The segmented image obtained by using our new model (iteration $= 10$, $\gamma = 100$, $\tau = 2$).

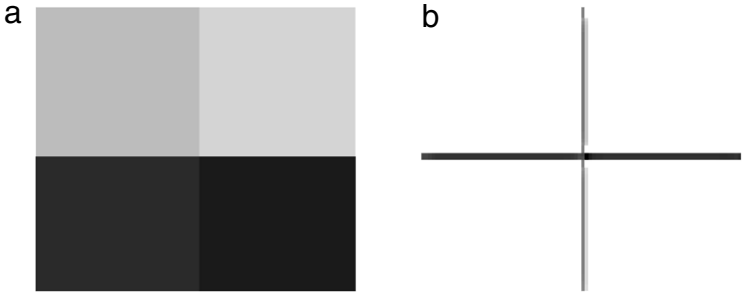

Fig. 4. An example of image segmentation: (a) The original image; (b) The segmented image obtained by using our new model (iteration $= 10$, $\gamma = 100$, $\tau = 2$).

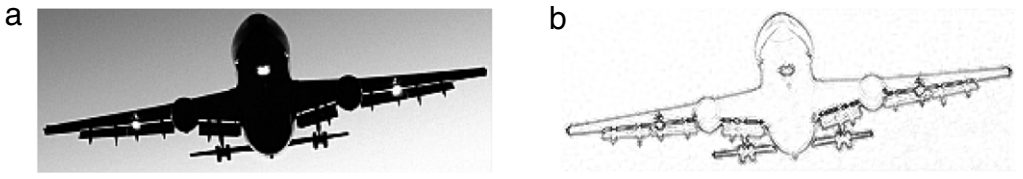

Fig. 5. An example of image segmentation: (a) The original image; (b) The segmented image obtained by using our new model (iteration $= 50$, $\gamma = 100$, $\tau = 2$).

In the following, we compare our proposed model with the model in [18] (see Figs. 6 and 7). Firstly, from Fig. 6, it is shown that our model can detect all the edges that cannot be found by using the model in [18].

Finally, we use the image of the cameraman Fig. 7(a) to compare our proposed model with the model in [18]. In the segmented image Fig. 7(b) obtained by our model, many details and edges could be detected. However, it is hard to achieve this result by using the model in [18].

6. Conclusion

This paper describes a new variational model for image segmentation. This new model is based on the complex Ginzburg–Landau model and the semi-norm defined by us. When dealing with gray images, our new models can perform

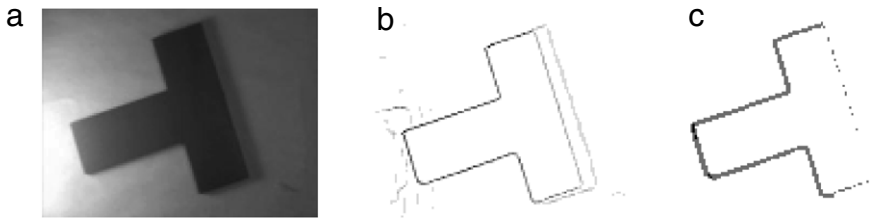

Fig. 6. An example of image segmentation: (a) The original image; (b) The segmented image obtained by using our new model (iteration $= 50$, $\gamma = 100$, $\tau = 2$); (c) The segmented image obtained by using the model in [18].

Fig. 7. An example of image segmentation: (a) The original image; (b) The segmented image obtained by using our new model (iteration $= 60$, $\gamma = 100$, $\tau = 2$); (c) The segmented image obtained by using the model in [18].

better than other methods, for example, fine structures can be kept better, the initialization is completely automatic and so on. Our experimental results confirm the effectiveness of our algorithm. Moreover, we have investigated some properties of our new semi-norm. However, it remains to conduct a complete theoretical study of the associated flows for our energy functionals. This will be our future work.

Acknowledgements

The authors express their deep thanks to the referees for their very helpful suggestions to improve some results in this paper.

References

[1] M. Kass, A. Witkin, D. Terzopoulos, Snakes: active contour models, Int. J. Comput. Vis. 1 (1988) 321–331.
[2] V. Caselles, R. Kimmel, G. Sapiro, Geodesic active contours, Int. J. Comput. Vis. 22 (1997) 61–79.
[3] C. Li, J. Liu, M.D. Fox, Segmentation of external force field for automatic initialization and splitting of snakes, Pattern Recognit. 38 (11) (2005) 1947–1960.
[4] C. Li, C. Xu, C. Gui, M.D. Fox, Level set evolution without re-initialization: a new variational formulation, in: IEEE Conference on Computer Vision and Pattern Recognition, CVPR, 2005, pp. 430–436.
[5] T. Chan, L. Vese, Active contours without edges, IEEE Trans. Image Process. 10 (2) (2001) 266–277.
[6] N. Paragios, R. Deriche, Geodesic active regions and level set methods for supervised texture segmentation, Int. J. Comput. Vis. 46 (2002) 223–247.
[7] A. Tsai, A. Yezzi, A.S. Willsky, Curve evolution implementation of the Mumford–Shah functional for image segmentation denoising interpolation and magnification, IEEE Trans. Image Process. 10 (2001) 1169–1186.
[8] L. Vese, T. Chan, A multiphase level set framework for image segmentation using the Mumford and Shah model, Int. J. Comput. Vis. 50 (2002) 271–293.
[9] C. Li, C. Kao, J.C. Gore, Z. Ding, Minimization of region-scalable fitting energy for image segmentation, IEEE Trans. Image Process. 17 (10) (2008) 1940–1949.
[10] V.L. Ginzburg, L.D. Landau, On the theory of superconductivity, Zh. Eksp. Teor. Fiz. 20 (1950) 1064–1082.
[11] G. Aubert, J.F. Aujol, L.B. Feraud, Detecting codimention two objects in an image with Ginzburg–Landau models, Int. J. Comput. Vis. 65 (2005) 29–42.
[12] A. Buades, B. Coll, J.M. Morel, A non-local algorithm for image denoising, in: Proceedings of IEEE Computer Society Conference on Computer Vision and Pattern Recognition, 2005, pp. 60–65.
[13] S. Kindermann, S. Osher, P.W. Jones, Deblurring and denoising of images by nonlocal functionals, SIAM J. Mult. Model. Sim. 4 (2005) 1091–1115.
[14] T.F. Chan, S. Osher, J. Shen, The digital TV filter and nonlinear denoising, IEEE Trans. Image Process. 10 (2) (2001) 231–241.
[15] Y. Chen, T. Wunderli, Adaptive total variation for image restoration in BV space, J. Math. Anal. Appl. 272 (2002) 117–137.
[16] S. Osher, A. Sole, L. Vese, Image decomposition and restoration using total variation minimization and the H.1 norm, SIAM J. Mult. Model. Sim. 1 (2003) 349–370.
[17] J.F. Aujol, A. Chambolle, Dual norms and image decomposition models, Int. J. Comput. Vis. 63 (1) (2005) 85–104.
[18] F. Li, C.M. Shen, L. Pi, A new diffusion-based variational model for image denoising and segmentation, J. Math. Imaging Vision 26 (2006) 115–125.